

Open Access:: ISSN 1847-9286 www.jESE-online.org

Original scientific paper

# Development of a non-invasive genosensor to diagnose pancreatic cancer using miRNA-196a

Namita Sharma and Sudha Srivastava<sup>™</sup>

Department of Biotechnology, Jaypee Institute of Information Technology, A-10, Sector-62, Noida, Uttar Pradesh, India

Corresponding author: Sudha.srivastava@jiit.ac.in; Tel.: +911202594212; Fax: +911202400986

Received: May 16, 2025; Accepted: September 8, 2025; Published: September 15, 2025

#### **Abstract**

This work presents the development of a diagnostic device for pancreatic cancer, one of the deadliest malignancies worldwide. The circulating pancreatic cancer biomarker miRNA-196a was utilized for the development of an electrochemical genosensor due to its stability in biological fluids. Immobilized single-stranded DNA conjugated with gold nanoparticles establishes a sensitive platform for the electrochemical detection of miRNA-196a. The sensor performance was evaluated for probe DNA-miRNA hybridization at optimum temperature (55 °C) using cyclic voltammetry and chronocoulometric techniques, achieving sensitivities of 51.10  $\mu$ A pg<sup>-1</sup> mL cm<sup>-2</sup> and 18.28  $\mu$ C pg<sup>-1</sup> mL cm<sup>-2</sup>, respectively. The device exhibited a wide linear detection range of miRNA-196a from 14.9 aM to 14.9 nM. To the best of our knowledge, for already developed PDAC biosensors using a single biomarker or a panel of biomarkers, the widest detection range for miRNA-196a was reported as 0.05 fM to 50 pM by Guo et al. in 2018. Hence, the developed genosensor, having a detection limit of 14.9 aM and a wide detection range, may prove to be a promising tool in detecting pancreatic cancer at an early stage, and hence improve patient outcomes.

#### **Keywords**

DNA biosensor; gold nanoparticles; hybridization; cyclic voltammetry; chronocoulometry; limit of detection

#### Introduction

Micro ribonucleic acid (miRNA) is a small, highly conserved, and non-coding RNA with 18 to 25 nucleotides, responsible for the regulation of several cellular functions. Their importance in cancer was highlighted in 2002 when Dr. Croce's group [1] demonstrated the involvement of miRNA in chronic lymphocytic leukaemia (CLL). They confirmed that during B-cell chronic lymphocytic leukaemia (B-CLL), miR-15 and miR-16 were downregulated due to the deletion of the 13q14 region of the chromosome, where both miRNAs were located [1]. Several studies also exhibited miRNA's role in the inhibition of tumour suppressor genes and genes that induce apoptosis during cancer [2,3]. The expression levels of miRNAs during cancer could be utilized for diagnostic, as well as prognostic,

disease-related miRNA biomarkers [4]. Body fluids such as blood, saliva, urine, tears, peritoneal fluid, colostrum, etc., with circulating miRNAs are considered useful biomarkers due to their stability and easy accessibility [2].

The expression level of miRNA-196a can discriminate between normal, chronic pancreatitis, benign pancreatic tumours, and pancreatic adenocarcinoma (PDAC) [5,6]. It was also reported that its expression levels are significantly higher in unresectable pancreatic cancer in stages III and IV compared to resectable instances in early stages I and II [7]. When compared to healthy individuals during the early stages of PDAC/pancreatic cancer, the plasma level was also found to be higher [8]. Besides this, miRNA-196a also regulates the genes responsible for its growth, invasion, and metastasis [2].

miR-196a has also been found to be upregulated in other cancers like gastric cancer [9], non-small cell lung cancer (NSCLC) [10], cervical cancer [11], breast cancer [12], liver cancer [13], esophageal squamous cell carcinoma (ESCC) [14], colorectal cancer [15], head and neck cancer [16], oral cancer [17], acute myeloid leukaemia [18] with the exception of renal cell carcinoma [19] and melanoma [20] where its expression is downregulated. However, its expression level is also elevated in several diseases, such as cerebral ischemia [21], Huntington's disease (HD) [22], and Crohn's disease [23], whereas it is low during Alzheimer's disease [24] and chronic hepatitis C infection (CHC) [25].

The current gold standard for pancreatic cancer diagnosis is endoscopic ultrasound-guided fine needle aspiration biopsy (EUS-FNAB) [26,27], although other techniques like computed tomography (CT) scan, magnetic resonance imaging (MRI), ultrasound, reverse transcription polymerase chain reaction (RT-PCR), next-generation sequencing (NGS) and microarrays have also been used. However, these techniques are costly, time-consuming, require sample pre-processing, and ample amounts of sample [28,29]. To address these constraints and enhance diagnostic effectiveness, electrochemical biosensors are considered as an alternative diagnostic platform [30]. They offer several advantages, including non-invasiveness, low cost, on-site analysis, small size, the ability to detect low amounts of circulating biomarkers, ease of handling, rapid response, and high sensitivity [31,32]. This genosensor generates a measurable electrical signal through the specific hybridization between the target nucleic acid present in the biological sample and a complementary synthetic probe designed against it. Such sensors could also be applied for detecting infectious diseases, genetic disorders, pathogens, etc. [32]. The nanomaterials, like metallic nanoparticles (gold, silver, copper, platinum, palladium, etc.) are used alone or in combination with some other metals and conducting polymers [33]. Thus, polyaniline, poly(phenylenevinylene), polypyrrole, poly(para-phenylene), and polythiophene are used in fabricating stable and sensitive devices that could detect markers at very low concentrations [34].

Several recent studies have demonstrated the effectiveness of sensors for detecting pancreatic cancer-related miRNAs and a panel of miRNA biomarkers. Al-Fandi and his team [35] developed a nanosensor using multi-walled carbon nanotubes and gold nanoparticles to detect miR-21 with a lower limit of detection of 3.68 femtomolar (fM). Chen and co-workers in 2020 [36] designed a polydopamine-gold composite and dual signal amplification strategy for the detection of miR-196b with a lower detection limit of 0.26 pM. Mi and his group [37] employed a DNA tetrahedral nanostructure to simultaneously detect multiple miRNAs-miR-155, miR-21, miR-196a and miR-210 from serum samples against pancreatic cancer. They detected these markers with a sensitivity of 10 fM [37]. In another study, Xiong with his team [38] developed a nanochannel-based biosensor to detect pancreatic cancer-specific miRNAs, *i.e.* miR-21, miR-155 and miR-196a on a single platform. Joshi and Waghmode [39] developed a sensor to detect the p16 gene with a detection ability of 0.10 pM.

In this study, we report the preparation and analytical properties of a highly sensitive electrochemical genosensor for the detection of miR-196a, with a detection limit as low as attomolar (aM) levels. The high sensitivity of the developed genosensor, achieved through the integration of nanomaterials and a screen-printed electrode, along with a probe immobilization strategy, enhances its analytical performance, making it a promising tool for the early diagnosis and prognosis of PDAC.

### **Experimental**

#### Chemicals

Oligonucleotides miRNA 196a and amino-labeled single-stranded DNA (ss-DNA probe 196a) were synthesized and purchased from Sigma-Aldrich. The sequences ssDNA probe and its complementary target miRNA-196a are:

Probe ssDNA (pr miR-196a) – 5' [AmC<sub>6</sub>] CCCAACAACATGAAACTACCTA3'

miRNA-196a - 5' UAGGUAGUUUCAUGUUGUUGGG 3'

Mismatch 1 (M1) – 5' UAGGUAAUUUCAUGUUGUUGGG 3'

Mismatch 2 (M2) – 5' UAGGUAACUCAUGUUGUUGGG 3'

Lyophilized solutions of these oligonucleotides (100  $\mu$ M) were resuspended in TE Buffer (0.01 M Tris-EDTA, pH 7.8) and stored at -20 °C (ssDNA) and -80 °C (miR-196a). Tetrachloroauric acid (HAuCl<sub>4</sub>·3H<sub>2</sub>O), cysteamine hydrochloride (CysHCl) (HSCH<sub>2</sub>CH<sub>2</sub>NH<sub>2</sub>·HCl), and trisodium citrate dihydrate (C<sub>6</sub>H<sub>5</sub>Na<sub>3</sub>O<sub>7</sub>·2H<sub>2</sub>O) were procured from Sigma-Aldrich. Potassium ferrocyanide [K<sub>4</sub>Fe(CN)<sub>6</sub>], potassium ferricyanide [K<sub>3</sub>Fe(CN)<sub>6</sub>], tris-(hydroxymethyl) aminomethane (Tris), and ethylenediamine-tetraacetic acid (EDTA), were purchased from Himedia Laboratories Pvt. Ltd. Sodium dihydrogen phosphate (NaH<sub>2</sub>PO<sub>4</sub>), disodium hydrogen phosphate (Na<sub>2</sub>HPO<sub>4</sub>), gelatin, and Tween 20 were purchased from CDH Chemicals. MilliQ water (18 M $\Omega$  cm<sup>-1</sup>) was used to prepare all buffer solutions.

#### Instrumentation

All electrochemical experiments were carried out on an electrochemical workstation, CHI604E (CH Instruments Inc., USA). The optical characterization of the synthesized gold nanoparticles was performed using a UV/Vis spectrophotometer (Jenway). The size and shape of the nanoparticles were determined using transmission electron microscopy (TALOS HR-TEM, AIIMS Delhi). Screen-printed electrodes (gold) were purchased from DTech Solutions, Kanpur. The working and counter electrodes were gold, and Ag/AgCl was used as a reference electrode. The working electrode diameter was 3 mm, 50 mm height and 13 mm width, defining the geometrical area of the working electrode as 0.0707 cm<sup>2</sup>.

### Synthesis of spherical gold nanoparticles

Citrate-capped gold nanoparticles were synthesized using the Turkevich method [40]. 3 mL of 100 mM trisodium citrate was added dropwise (0.1 mL min $^{-1}$ ) into a solution of 5 mM (2 mL) trichloroauric acid prepared in 100 mL of boiling water. The reaction mixture was maintained at boiling conditions and continuously stirred using a magnetic stirrer. The formation of gold nanoparticles appeared gradually through the colour change from pale yellow to red. The colloidal solution was quenched by quickly placing it on the ice. The obtained solution was centrifuged after sonication at 9000 rpm for 15 min. The obtained nanoparticle pellets were resuspended in 100  $\mu$ L Milli-Q water.

## Fabrication of genosensor

The working surface of the screen-printed gold electrode (SPGE) was modified to develop a miRNA-based electrochemical biosensor. Firstly, the electrode was cleaned by using 70 % ethanol to remove impurities, followed by rinsing it with Milli-Q water 3-4 times. The monolayer of cysteamine hydrochloride was formed after the addition of 5  $\mu$ L of 2 mg mL<sup>-1</sup> over the working surface, after providing incubation for 1 hr under dark conditions. Then, the prepared SPGE/CysHCl

was washed and dried, and 5  $\mu$ L of gold nanoparticles(optical density 1.0) were added over the CysHCl layer and again incubated for 1 hr under ambient conditions, forming SPGE/CysHCl/AuNPs. Furthermore, 0.5  $\mu$ g of amino-labelled ssDNA probe, prepared in TE buffer (pH 7.8), was immobilized over the previously formed nanoparticle layer and further incubated for 1 h at room temperature. After this step, the exposed surface of SPGE/CysHCl/AuNPs/DNA electrode was blocked by using gelatine prepared in 0.1 % Tween 20, with phosphate buffer (PB) (0.01 M, pH 7.4) as a blocking agent, giving the final genosensor electrode, SPGE/CysHCl/AuNPs/DNA/gelatine. The layers formed over the electrode after each modification step form a covalent linkage with each other to provide stability. Cyclic voltammetry (CV) was performed after each step of modification.

## Optimization of hybridization temperature

After the fabrication of SPGE/CysHCl/AuNPs/DNA/gelatine, the hybridization temperature was optimized to attain high binding efficiency. The optimum temperature was obtained after incubating 5 ng mL<sup>-1</sup> of complementary miRNA-196a at different temperatures, 37, 45, 50, 55 and 60 °C. The melting temperature of miR-196a is 60.3 °C. The cyclic voltammetry was performed to obtain the change in current response before and after hybridization. Different electrodes for the various temperatures were evaluated after 2 minutes (120 seconds) of incubation.

#### Electrochemical measurements

The fabricated electrode was characterized by performing cyclic voltammetry scanning from -0.8 to +0.8 V at a rate of  $0.1 \text{ V s}^{-1}$  after each modification step. The response of the genosensor, SPGE/CysHCl//AuNPs/DNA/gelatine, was tested after incubating different concentrations of miRNA-196a (0.0001, 0.05, 0.1, 50, 100, 50,000 and 100,000 pg mL<sup>-1</sup>) at the optimum temperature by cyclic voltammetry (CV) and chronocoulometric (CC) methods. The chronocoulometric response was obtained in two steps and carried out from -0.8 to +0.8 V, with a pulse width of 0.25 s. All electrochemical measurements were taken with a 5 mM ferri-ferrocyanide solution in 0.1 M KCl prepared in 0.1 M phosphate buffer (pH 7.4). The sensitivity of the developed genosensor was calculated using Equation (1):

Sensitivity = 
$$\frac{\text{slope of the linear region}}{\text{area of working electrode}}$$
 (1)

## **Results and discussion**

Characterization of spherical gold nanoparticles

The synthesis of colloidal gold nanoparticles was verified by UV-visible spectrum ( $\lambda_{max}$  = 521 nm), which was further confirmed by TEM, as shown in Figure 1.

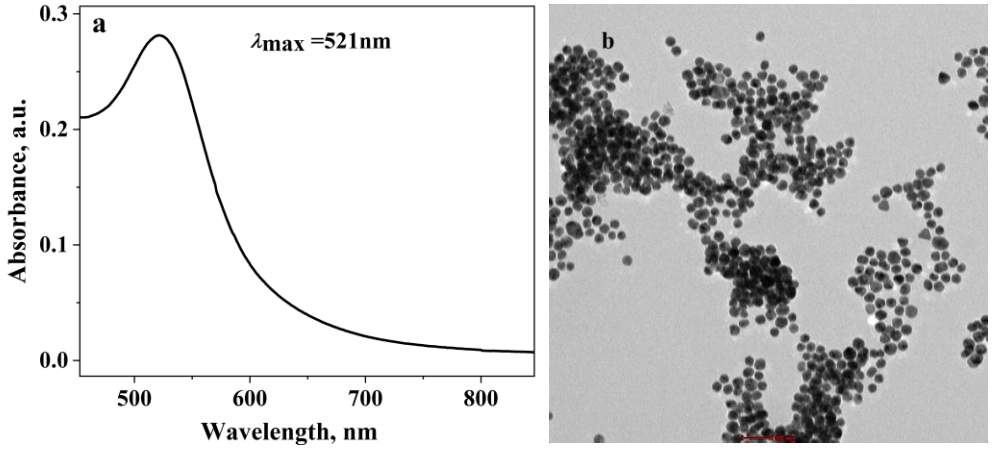
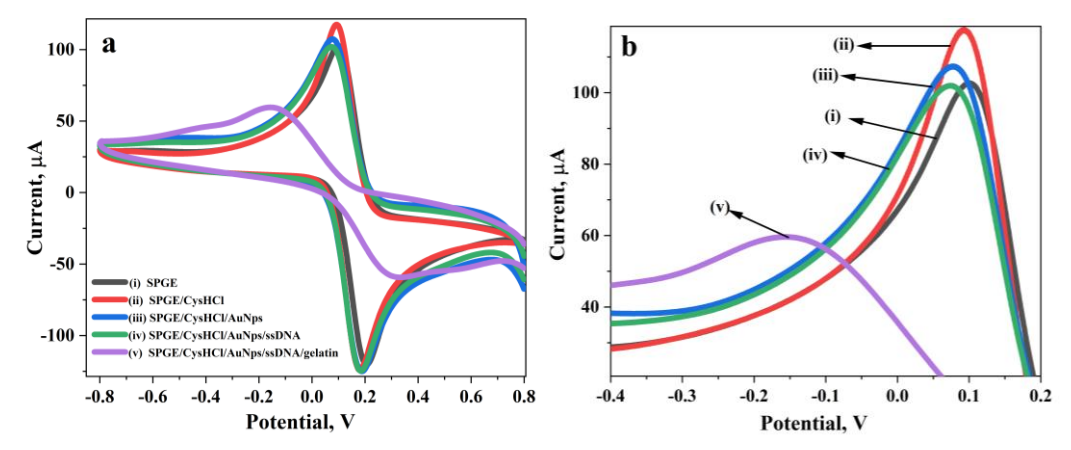


Figure 1. Characterization of gold nanoparticles: (a) UV-visible spectrum; (b) TEM image

## Electrochemical characterization of modified screen-printed gold electrode

The screen-printed gold electrode (SPGE) after various steps of modification was electrochemically characterized by cyclic voltammetry (CV) performed in 0.1 M KCl/0.1 M phosphate buffer (pH 7.4), containing 5 mM of Fe(CN) $_6$ ] $^{3-/4-}$  redox couple. Different modification steps of SPGE were identified through changes in potential and current values (Figure 2).



**Figure 2.** Characterization of a fabricated SPGE at different (i-v) steps of modification in 0.1 M KCl/0.1 M phosphate buffer (pH 7.4) with 5 mM of Fe(CN) $_6$ ]<sup>3-/4-</sup>: (a) cyclic voltammograms (0.1 V s<sup>-1</sup>) from -0.8 to +0.8 V and (b) enlarged CVs from -0.4 to 0.2 V

The formation of a self-assembled monolayer of CysHCl over the working surface of the bare electrode was confirmed through the slight shift of anodic peak potential ( $E_{pa}$ ) from 0.100 to 0.092 V and an increase in anodic peak current ( $I_{pa}$ ) from 102.69 to 117.49  $\mu$ A (red curve on Figure 2.). This is due to the positive charges provided by the terminal amine groups of CysHCl (HSCH<sub>2</sub>CH<sub>2</sub>NH<sub>2</sub>·HCl) over the surface of the electrode, allowing the unhindered movement of [Fe(CN)<sub>6</sub>]<sup>-3/-4</sup> ions to the electrode surface. The decrease in anodic peak potential ( $E_{pa}$ ) from 0.092 to 0.077 V and anodic peak current  $(I_{pa})$  from 117.49 to 107.32  $\mu$ A (blue curve) was observed after the electrode was functionalized by citrate-capped gold nanoparticles. This may be due to the carboxyl groups of nanoparticles reacting to form covalent bonding with the amine groups of CysHCl. Further, the immobilization of the singlestranded DNA probe was accomplished by the formation of a covalent bond with the carboxyl group of nanoparticles and confirmed through a change in anodic peak potential from 0.077 to 0.073 V and anodic peak current from 107.32 to 101.95 µA (green curve). The upright ssDNA configuration is now allowed to bind with its complementary miRNA-196a. The exposed surface of the working electrode was blocked to avoid non-specific interactions by using a blocking buffer. The blocking of the surface was validated through the change in anodic peak potential from 0.073 to -0.152 V and anodic peak current from 101.95 to 59.51 µA (purple curve).

### Optimization of hybridization temperature

The binding efficiency of the single-stranded DNA (ssDNA) probe towards its complementary target miRNA-196a was analysed after incubation at different temperatures, 37, 45, 50, 55 and 60 °C. As shown in Figure 3, the maximum change in the cathodic current response after hybridization of 5 ng mL<sup>-1</sup> target miRNA-196a with probe DNA at modified SPGE was recorded at 55 °C. Therefore, to check the analytical response of the genosensor, hybridization (DNA-miRNA196a) at the optimum temperature of 55°C and incubation time of 120 s was used in all cyclic voltammetric and chronocoulometric experiments. This showed that at higher temperatures, the target miRNA unfolds and binds with the DNA probe, providing higher hybridization efficiency. Flechsig and Reske [41] have found an enhanced signal after hybridization at 50 °C when compared to 23 °C.

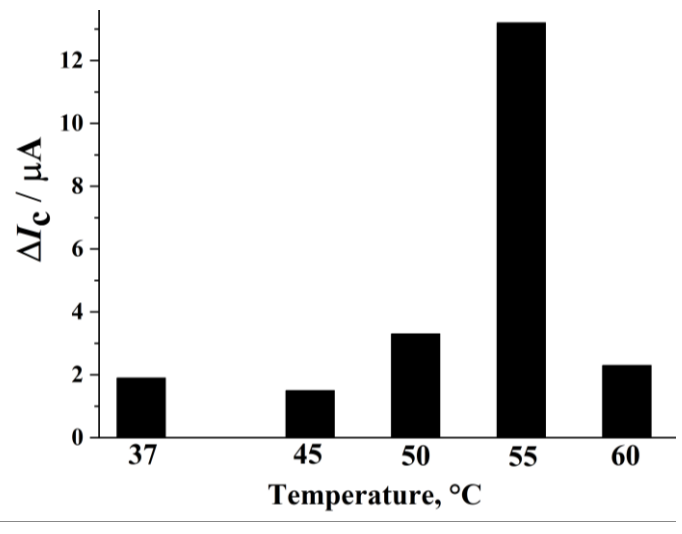


**Figure 3.** Influence of temperature of miRNA-196a hybridization with DNA probe on the change of cathodic peak current ( $\Delta I_c$ ), where  $\Delta I_c$  is cathodic current after DNA-miRNA196a hybridization – cathodic current before addition of miR196a sample

## Electrochemical response of the genosensor

CV response of the fabricated genosensor electrode, SPGE/CysHCl/AuNPs/DNA/gelatine, was obtained after hybridizing the probe (ssDNA) with its target miR-196a at 55 °C for 120 s. The efficient binding after hybridization over the electrode surface was analysed through current response with increasing concentrations (0.0001 to 100,000 pg mL<sup>-1</sup>) of miRNA-196a (Figure 4(a)). The decrease in oxidation and reduction peak current after probe DNA-miRNA196a hybridization and shifts in peak potentials (reduction and oxidation) with increasing concentrations of miR-196a were observed. These might be due to the accumulation of negative charges over the electrode surface after nucleic acid hybridization. The accumulated negative charges over the electrode surface hinder the electron transfer of redox species to the electrode, thus reducing the current response. The linear relationship of cathodic or reduction current ( $I_c$ ) was obtained. The calibration plot was plotted as reduction current at potential 0.23 V against the logarithm of miR-196a concentrations, as shown in Figure 4(b). The linear regression equation obtained was y = 3.61x - 68.40 with the correlation coefficient ( $R^2$ ) of 0.97, where x is the logarithm concentration of miRNA-196a (log C).

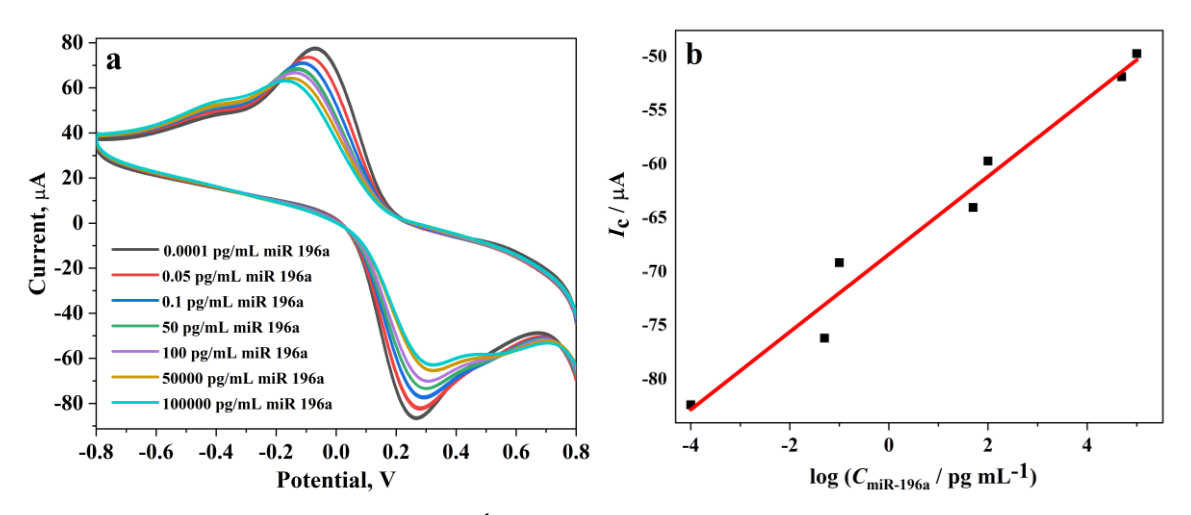


**Figure 4.** (a) Cyclic voltammograms (0.1 V s<sup>-1</sup>) of the fabricated genosensor electrode after incubating at 55 °C in 0.1 M KCl / 0.1 M phosphate buffer (pH 7.4) with 5 mM of Fe(CN)<sub>6</sub>]<sup>-3/-4</sup> and increasing concentrations of miR-196a (0.0001 to 100,000 pg mL<sup>-1</sup>); b) calibration plot of cathodic current at 0.23 V as a function of log ( $C_{miR-196a}$ )

The linear range was found to be 0.0001 to 100,000 pg mL-1 (14.9 aM to 14.9 nM) for miR-196a, with the sensitivity of  $51.10~\mu\text{A}$  pg<sup>-1</sup> mL cm<sup>-2</sup>, which was calculated using equation (1). The detection limit obtained was 14.9 aM. Similarly, Guo *et al.* [42] developed a biosensor against miR-196a, which exhibited a linear range from 0.05 fM to 50 pM, with a detection limit of 15 aM. Another study by Chen and co-workers [36] on miRNA-196b, a pancreatic biomarker, showed a detection limit of 0.26 pM, which is higher than that obtained from our developed genosensor.

Chronocoulometric (CC) measurements were also performed at the optimum temperature to analyse and quantify the charge response after hybridization. CC curves displayed a decrease in charge with increasing concentrations of miRNA-196a (0.0001 to 100,000 pg mL<sup>-1</sup>) as depicted in Figure 5(a).

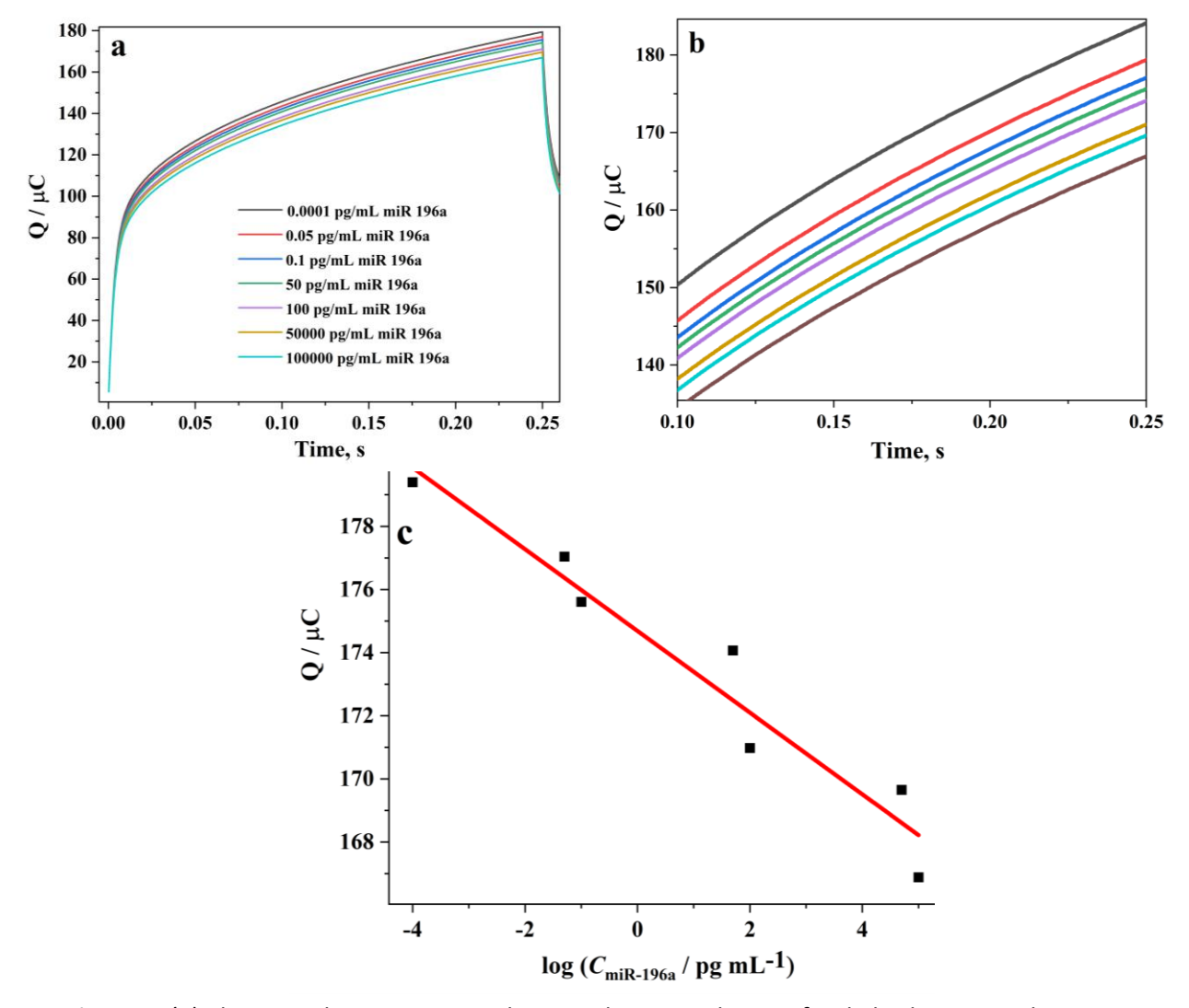


**Figure 5.** (a) Chronocoulometric curves showing change in charge after hybridization with increasing concentrations of miR 196a (0.0001 to 100,000 pg mL $^{-1}$ ) after incubating at 55 °C, (b) enlarged CC curves from t = 0.10 to 0.25 s, (c) calibration plot

The magnified CC curve from 0.10 to 0.25 s is displayed in Figure 5(b). The value of the change in the charge with increasing miR-196a concentrations was calculated at t = 0.25 s. The calibration plot was plotted as charge (Q) against logarithmic concentration of miR-196a. The linear regression equation was determined as y = 1.29x + 174.68 with  $R^2 = 0.93$ . The linear range was obtained from 0.0001 to 100,000 pg mL<sup>-1</sup> (14.9 aM to 14.9 nM) for miR-196a with a sensitivity of 18.28  $\mu$ C pg<sup>-1</sup> mL cm<sup>-2</sup>. The detection limit obtained was 14.9 aM (Figure 5(c)).

## Specificity of genosensor

To examine the specificity of the developed genosensor, its response was evaluated against a single-base mismatch sequence (M1) and a double-base mismatch sequence (M2), as illustrated in Figure 6. Cyclic voltammetry was used to analyse the sensor's ability to discriminate between fully complementary and mismatched sequences. Hybridization with non-complementary sequences showed signal interference of 19.4 % from M1 and 22 % from M2, demonstrating minimal hybridization. The observed interference percentages fall within or near the internationally accepted threshold range of 15 to 20 %, demonstrating reliable sequence selectivity of the genosensor [43].

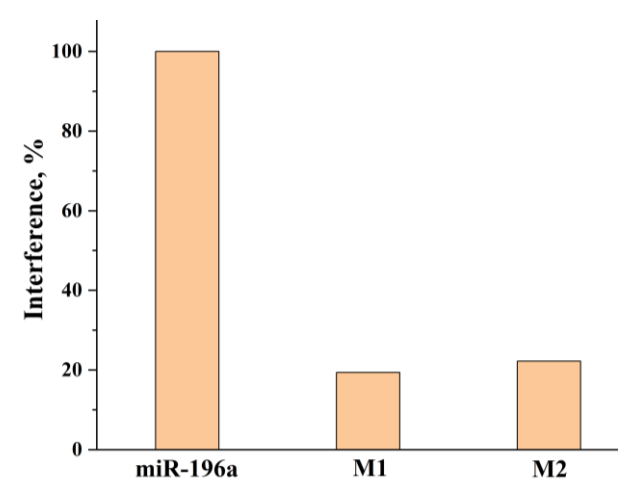


**Figure 6.** Comparison of interferences obtained from M1 (single base mismatch), M2 (double-base mismatch) against the complementary miR-196a

### **Conclusions**

In this study, we developed a non-invasive electrochemical genosensor for detecting miRNA-196a, a marker for pancreatic cancer. Electrochemical measurements through cyclic voltammetry provide a sensitivity of  $51.10~\mu\text{A}$  pg $^{-1}$  mL cm $^{-2}$  and  $18.28~\mu\text{C}$  pg $^{-1}$  mL cm $^{-2}$  through chronocoulometric analysis, at 55~°C. The genosensor achieved a low limit of detection (LOD) of 14.9 aM, indicating its capability to detect low levels of miRNA-196a. These findings highlight the potential of sensors as a rapid, low-cost, and highly sensitive diagnostic platform for the early detection. The non-invasive nature of the device made it a valuable tool for screening and point-of-care applications. Such advancements could contribute significantly to improved early diagnosis, better patient outcomes, and more effective management of pancreatic and other miRNA-associated cancers.

**Acknowledgements:** Namita is thankful to Jaypee Institute of Information Technology, Noida, India, for providing a research fellowship and other research facilities for the completion of this project. The authors are also thankful to AIIMS, Delhi, for the advanced instrumentation and research facility for transmission electron microscopy analysis.

**Conflict of interest:** There are no conflicts of interest to declare

### References

- [1] G. A. Calin, C. D. Dumitru, M. Shimizu, R. Bichi, S. Zupo, E. Noch, H. Aldler, S. Rattan, M. Keating, K. Rai, L. Rassenti, T. Kipps, M. Negrini, F. Bullrich, C.M. Croce, Frequent deletions and down-regulation of micro-RNA genes miR15 and miR16 at 13q14 in chronic lymphocytic leukemia, Proceedings of the National Academy of Sciences (PNAS) 99 (2002) 15524-15529. https://doi.org/10.1073/pnas.242606799
- [2] R. A. Subramani, L. Gangwani, S. B. Nandy, A. Arumugam, M. Chattopadhyay, R. Lakshmanaswamy, Emerging roles of microRNAs in pancreatic cancer diagnosis, therapy and prognosis, *International Journal of Oncology* **47** (2015) 1203-1210. https://doi.org/10.3892/ijo.2015.3129



- [3] B. Smolarz, A. Durczyński, H. Romanowicz, K. Szyłło, P. Hogendorf, miRNAs in Cancer (Review of Literature), *International Journal of Molecular Science* 23 (2022) 2805. https://doi.org/10.3390/ijms23052805
- [4] Y. Peng, C. M. Croce, The role of MicroRNAs in human cancer, *Signal Transduction and Targeted Therapy* **1** (2016) 15004. https://doi.org/10.1038/sigtrans.2015.4
- [5] M. Liu, Y. Du, J. Gao, J. Liu, X. Kong, Y. Gong, Z. Li, H. Wu, H. Chen, Aberrant expression miR-196a is associated with abnormal apoptosis, invasion, and proliferation of pancreatic cancer cells, *Pancreas* **42** (2013) 1169-1181. <a href="https://doi.org/10.1097/MPA.0b013e3182962acb">https://doi.org/10.1097/MPA.0b013e3182962acb</a>
- [6] M. Bloomston, W. L. Frankel, F. Petrocca, S. Volinia, H. Alder, J. P. Hagan, C. G. Liu, D. Bhatt, C. Taccioli, C. M. Croce, MicroRNA expression patterns to differentiate pancreatic adenocarcinoma from normal pancreas and chronic pancreatitis, *Jama* 297 (2007) 1901-1918. https://doi.org/10.1001/jama.297.17.1901
- [7] F. Huang, J. Tang, X. Zhuang, Y. Zhuang, W. Chen, W. Chen, H. Yao, S. Zhang, MiR-196a promotes pancreatic cancer progression by targeting nuclear factor kappa-B-inhibitor alpha, *PloS One* **9** (2014) e87897. <a href="https://doi.org/10.1371/journal.pone.0087897">https://doi.org/10.1371/journal.pone.0087897</a>
- [8] A. A Tesfaye, A. S Azmi, P. A. Philip, miRNA and gene expression in pancreatic ductal adenocarcinoma, *The American Journal of Pathology* **189** (2019) 58-70. <a href="https://doi.org/10.1016/j.ajpath.2018.10.005">https://doi.org/10.1016/j.ajpath.2018.10.005</a>
- [9] M. Sun, X. -H. Liu, J. -H. Li, J. -S. Yang, E. -B. Zhang, D. -D. Yin, Z. -L. Liu, J. Zhou, Y. Ding, S. -Q. Li, Z. -X. Wang, X. -F. Cao, W. De, MiR-196a is upregulated in gastric cancer and promotes cell proliferation by downregulating p27kip1, *Molecular Cancer Therapeutics* 11 (2012) 842-852. <a href="https://doi.org/10.1158/1535-7163.MCT-11-1015">https://doi.org/10.1158/1535-7163.MCT-11-1015</a>
- [10] Q. Li, Z. Yang, M. Chen, Y. Liu, Downregulation of microRNA-196a enhances the sensitivity of non-small cell lung cancer cells to cisplatin treatment, *International Journal of Molecular Medicine* **37** (2016) 1067-1074. https://doi.org/10.3892/ijmm.2016.2513
- [11] J. Li, Q. Liu, L. H. Clark, H. Qiu, V. L. Bae-Jump, C. Zhou, Deregulated miRNAs in human cervical cancer: functional importance and potential clinical use, *Future Oncology* **13** (2016) 743-753. https://doi.org/10.2217/fon-2016-0328
- [12] Q. Han, C. Zhou, F. Liu, G. Xu, R. Zheng, X. Zhang, MicroRNA-196a post-transcriptionally upregulates the UBE2C proto-oncogene and promotes cell proliferation in breast cancer, *Oncology Reports* 34 (2015) 877-883. <a href="https://doi.org/10.3892/or.2015.4049">https://doi.org/10.3892/or.2015.4049</a>
- [13] L. Yang, F. Peng, J. Qin, H. Zhou, B. Wang, Downregulation of microRNA-196a inhibits human liver cancer cell proliferation and invasion by targeting FOXO1, *Oncology Reports* **38** (2017) 2148-2154. <a href="https://doi.org/10.3892/or.2017.5873">https://doi.org/10.3892/or.2017.5873</a>.
- [14] C. Hu, J. Peng, L. Lv, X. Wang, Y. Zhou, J. Huo, D. Liu, miR-196a regulates the proliferation, invasion and migration of esophageal squamous carcinoma cells by targeting ANXA1, *Oncology Letters* **17** (2019) 5201-5209. <a href="https://doi.org/10.3892/ol.2019.10186">https://doi.org/10.3892/ol.2019.10186</a>
- [15] J. Ge, Z. Chen, R. Li, T. Lu, G. Xiao, Upregulation of microRNA-196a and microRNA-196b cooperatively correlate with aggressive progression and unfavorable prognosis in patients with colorectal cancer, *Cancer Cell International* **14** (2014) 128. https://doi.org/10.1186/s12935-014-0128-2
- [16] Y. E. Suh, N. Raulf, J. Gäken, K. Lawler, T. G. Urbano, J. Bullenkamp, S. Gobeil, J. Huot, E. Odell, M. Tavassoli, MicroRNA-196a promotes an oncogenic effect in head and neck cancer cells by suppressing annexin A1 and enhancing radioresistance, *International Journal of Cancer* 137 (2015) 1021-1034. <a href="https://doi.org/10.1002/ijc.29397">https://doi.org/10.1002/ijc.29397</a>
- [17] Y. -C. Lu, J. T. Chang, C. -T. Liao, C. -J. Kang, S. -F. Huang, I. -H. Chen, C. -C. Huang, Y. -C. Huang, W. -H. Chen, C. -Y. Tsai, H. -M. Wang, C. -H. Yen, G. -R. You, C. -H. Chiang, A. -J. Cheng, OncomiR-196 promotes an invasive phenotype in oral cancer through the NME4-JNK-TIMP1-MMP signaling pathway, *Molecular Cancer* 13 (2014) 218. https://doi.org/10.1186/1476-4598-13-218
- [18] E. Coskun, E. K. von der Heide, C. Schlee, A. Kühnl, N. Gökbuget, D. Hoelzer, W. -K. Hofmann, E. Thiel, C. D. Baldus, The role of microRNA-196a and microRNA-196b as ERG regulators in acute myeloid leukemia and acute T-lymphoblastic leukemia, *Leukemia Research* 35 (2011) 208-213. <a href="https://doi.org/10.1016/j.leukres.2010.05.007">https://doi.org/10.1016/j.leukres.2010.05.007</a>
- [19] Y. Li, L. Jin, D. Chen, J. Liu, Z. Su, S. Yang, Y. Gui, X. Mao, G. Nie, Y. Lai, Tumor suppressive miR-196a is associated with cellular migration, proliferation and apoptosis in renal cell carcinoma, *Molecular Medicine Reports* **14** (2016) 560-566. <a href="https://doi.org/10.3892/mmr.2016.5251">https://doi.org/10.3892/mmr.2016.5251</a>

- [20] S. Braig, D. W. Mueller, T. Rothhammer, A.-K. Bosserhoff, MicroRNA miR-196a is a central regulator of HOX-B7 and BMP4 expression in malignant melanoma: PP54, *Pigment Cell & Melanoma Research* **22** (2009) 695. <a href="https://doi.org/10.1007/s00018-010-0394-7">https://doi.org/10.1007/s00018-010-0394-7</a>
- [21] D. -L. Zhang, X. Liu, Q. Wang, N. LI, S. -H. Wu, C. Wang, Downregulation of microRNA-196a attenuates ischemic brain injury in rats by directly targeting HMGA1, *European Review for Medical & Pharmacological Sciences* **23** (2019) 740-748. <a href="https://doi.org/10.26355/eurrev">https://doi.org/10.26355/eurrev</a> 201901 16888
- [22] X. Dong, S. Cong, MicroRNAs in Huntington's disease: diagnostic biomarkers or therapeutic agents?, *Frontiers in Cellular Neuroscience* **15** (2021) 705348. <a href="https://doi.org/10.3389/fncel.2021.705348">https://doi.org/10.3389/fncel.2021.705348</a>
- [23] P. Brest, P. Lapaquette, M. Souidi, K. Lebrigand, A. Cesaro, V. Vouret-Craviari, B. Mari, P. Barbry, J. F. Mosnier, X. Hébuterne, A. Harel-Bellan, B. Mograbi, A. Darfeuille-Michaud, P. Hofman, A synonymous variant in IRGM alters a binding site for miR-196 and causes deregulation of IRGM-dependent xenophagy in Crohn's disease, *Nature Genetics* **43** (2011) 242-245. <a href="https://doi.org/10.1038/ng.762">https://doi.org/10.1038/ng.762</a>
- [24] K. Yang, S. Feng, J. Ren, W. Zhou, Upregulation of microRNA-196a improves cognitive impairment and alleviates neuronal damage in hippocampus tissues of Alzheimer's disease through downregulating LRIG3 expression, *Journal of Cellular Biochemistry* 120 (2019) 17811-17821. <a href="https://doi.org/10.1002/jcb.29047">https://doi.org/10.1002/jcb.29047</a>
- [25] B. Liu, Y. Xiang, H. S. Zhang, Circulating microRNA-196a as a candidate diagnostic biomarker for chronic hepatitis C, *Molecular Medicine Reports* **12** (2015) 105-110. <a href="https://doi.org/10.3892/mmr.2015.3386">https://doi.org/10.3892/mmr.2015.3386</a>
- [26] N. Fujimor, Y. Minoda, Y. Ogawa, What is the best modality for diagnosing pancreatic cancer, *Digestive Endoscopy* **34** (2022) 744–746. https://doi.org/10.1111/den.14283
- [27] J. Yang, R. Xu, C. Wang, J. Qiu, B. Ren, L. You, Early screening and diagnosis strategies of pancreatic cancer: a comprehensive review, *Cancer Communications (London, England)* **41** (2021) 1257–1274. <a href="https://doi.org/10.1002/cac2.12204">https://doi.org/10.1002/cac2.12204</a>
- [28] E. Buscail, C. Maulat, F. Muscari, L. Chiche, P. Cordelier, S. Dabernat, C. Alix-Panabières, L. Buscail, Liquid biopsy approach for pancreatic ductal adenocarcinoma, *Cancers* 11 (2019) 852. <a href="https://doi.org/10.3390/cancers11060852">https://doi.org/10.3390/cancers11060852</a>
- [29] S. Kreth, M. Hübner, L. C. Hinske, MicroRNAs as clinical biomarkers and therapeutic tools in perioperative medicine, *Anesthesia & Analgesia* **126** (2018) 670-681. https://doi.org/10.1213/ANE.0000000000002444
- [30] T. F. H. Lestari, I. Irkham, U. Pratomo, S. Gaffar, S. N. Zakiyyah, I. Rahmawati, S.N. Topkaya, Y.W. Hartati, Label-free and label-based electrochemical detection of disease biomarker proteins, *ADMET & DMPK* **12** (2024) 463-486. https://doi.org/10.5599/admet.2162
- [31] X. Dong, X. Lu, K. Zhang, Y. Zhang, Chronocoulometric DNA biosensor based on a glassy carbon electrode modified with gold nanoparticles, poly (dopamine) and carbon nanotubes, *Microchimica Acta* **180** (2013) 101-108. <a href="https://doi.org/10.1007/s00604-012-0900-8">https://doi.org/10.1007/s00604-012-0900-8</a>
- [32] S. Campuzano, P. Yáñez-Sedeño, J. M. Pingarrón, Electrochemical genosensing of circulating biomarkers, *Sensors* **17** (2017) 866. <a href="https://doi.org/10.3390/s17040866">https://doi.org/10.3390/s17040866</a>
- [33] K. Namsheer, C. S. Rout, Conducting polymers: a comprehensive review on recent advances in synthesis, properties and applications, *RSC Advances* **11** (2021) 5659-5697. https://doi.org/10.1039/d0ra07800j
- [34] G. Paimard, E. Ghasali, M. Baeza, Screen-printed electrodes: Fabrication, modification, and biosensing applications, *Chemosensors* **11** (2023) 113. <a href="http://dx.doi.org/10.3390/chemosensors11020113">http://dx.doi.org/10.3390/chemosensors11020113</a>
- [35] I. Rawashdeh, M. G. Al-Fandi, Y. Makableh, T. Harahsha, Developing a nano-biosensor for early detection of pancreatic cancer, *Sensor Review* **41** (2021) 93-100. https://doi.org/10.1108/SR-01-2020-0004
- [36] S. C. Chen, K. T. Chen, A. F. Jou, Polydopamine-gold composite-based electrochemical biosensor using dual-amplification strategy for detecting pancreatic cancer-associated microRNA, *Biosensors and Bioelectronics* **173** (2021) 112815. https://doi.org/10.1016/j.bios.2020.112815
- [37] D. Zeng, Z. Wang, Z. Meng, P. Wang, L. San, W. Wang, A. Aldalbahi, L. Li, J. Shen, X. Mi, DNA Tetrahedral Nanostructure-Based Electrochemical miRNA Biosensor for Simultaneous Detection of Multiple miRNAs in Pancreatic Carcinoma, ACS Applied Materials & Interfaces 28 (2017) 24118-24125. <a href="https://doi.org/10.1021/acsami.7b05981">https://doi.org/10.1021/acsami.7b05981</a>
- [38] J. Xu, K. Liao, Z. Fu, Z. Xiong, A new method for early detection of pancreatic cancer biomarkers: detection of microRNAs by nanochannels, *Artificial Cells, Nanomedicine, and Biotechnology* **47** (2019) 2634-2640. <a href="http://dx.doi.org/10.1080/21691401.2019.1614594">http://dx.doi.org/10.1080/21691401.2019.1614594</a>



- [39] P. N. Joshi, S. Waghmode, Graphene quantum dot-based on-chip electrochemical DNA hybridization sensor for pancreatic cancer, *Reports in Electrochemistry* **14** (2016) 31-40. https://doi.org/10.2147/RIE.S83253
- [40] J. Turkevich, P. C. Stevenson, J. Hillier, A study of the nucleation and growth processes in the synthesis of colloidal gold, *Discussions of the Faraday Society* **11** (1951) 55-75. https://doi.org/10.1039/DF9511100055
- [41] G. U. Flechsig, T. Reske, Electrochemical detection of DNA hybridization by means of osmium tetroxide complexes and protective oligonucleotides, *Analytical Chemistry* **79** (2007) 2125-2130. https://doi.org/10.1021/ac062075c
- [42] J. Guo, C. Yuan, Q. Yan, Q. Duan, X. Li, G. Yi, An electrochemical biosensor for microRNA-196a detection based on cyclic enzymatic signal amplification and template-free DNA extension reaction with the adsorption of methylene blue, *Biosensors and Bioelectronics* **105** (2018) 103-108. http://dx.doi.org/10.1016/j.bios.2020.112815
- [43] N. Jendrike, A. Baumstark, U. Kamecke, C. Haug, G. Freckmann, ISO 15197: 2013 evaluation of a blood glucose monitoring system's measurement accuracy, *Journal of Diabetes Science and Technology* **11** (2017) 1275-1276. <a href="http://dx.doi.org/10.1177/1932296817727550">http://dx.doi.org/10.1177/1932296817727550</a>

©2025 by the authors; licensee IAPC, Zagreb, Croatia. This article is an open-access article distributed under the terms and conditions of the Creative Commons Attribution license (<a href="https://creativecommons.org/licenses/by/4.0/">https://creativecommons.org/licenses/by/4.0/</a>)